# THE INITIAL ORBIT DETERMINATION OF LEO SATELLITES OBSERVED NEAR THE LOCAL ZENITH

**M.A. Earl (a)**
*(a) Royal Military College of Canada, Kingston ON, earl-m@castor2.ca*

## Abstract

*Our large satellite population continues to rise due to an increasing launch frequency, on-orbit explosions, on-orbit collisions, and successful anti-satellite missile tests. Space situational awareness requires space science professionals who are highly skilled in space surveillance and astrodynamics. Typically, such subjects are introduced to undergraduate or graduate students; however, secondary school students with an aptitude in science and algebra can be introduced to basic space surveillance and astrodynamics concepts, in a way that provides a head start to studying problems associated with satellite overpopulation and space debris management. This paper proposes a method of initial orbit determination which can determine a low Earth orbiting satellite's orbit radius, inclination, and right ascension of the ascending node from a single image obtained of the local zenith. This "Zenith Method" introduces secondary school students to the basic concepts and difficulties that are associated with space surveillance and astrodynamics.*

## I Introduction

Space surveillance refers to propagating satellite orbit elements, known as Two-Line Element Sets (TLEs), which serve to locate and track satellites, and to determine satellites' orbit elements from the resulting tracking data. Some might assume that space surveillance can be performed using only complex and very expensive equipment. Although this is true in cases where highly accurate orbit elements of very small or low reflectance satellites is required, the availability of inexpensive, retail astronomical detectors, such as charge-coupled devices (CCDs) and computerized goto[1] telescopes has allowed backyard amateur astronomers to perform space surveillance inexpensively.

On any clear night, a number of low Earth orbit (LEO) satellites can be detected with the naked eye for up to two hours after evening twilight or for up to two hours before dawn. A CCD camera fitted with a small camera lens can detect fainter, and therefore a larger number, of LEOs within the same time. Most of the detected LEO satellites will be within 1,000km in altitude or within 7,400km from the Earth's center[2].

If a satellite is observed to traverse the sky over its entire pass (assuming no eclipses), it will appear to move very slowly near the horizon and much faster near the local zenith. This is mainly due to the constantly varying observed transverse component of the orbit's tangential (along-track) velocity vector. When observed close to the horizon, most of the satellite's velocity will be moving away or toward the observer's location. The velocity's radial component will, in this case, be much larger than its observed transverse component. When observed near zenith, the satellite velocity's transverse component will be much larger than its radial component. In this case, the velocity's transverse component will be nearly equal to the satellite's tangential orbit velocity, unless the satellite has a high orbit eccentricity, or unless the satellite's orbit radius is large enough such that the Earth's rotational velocity is comparable in magnitude [1].

Provided that a LEO satellite is bright enough to be detected, when imaged with a camera, a suitable time exposure (integration time) will result in a star field background with a streak. The streak depicts the

[1] "Goto" refers to an ability to point to a celestial object at the push of a button or command from a computer.
[2] Assuming that Earth's gravitational and geometric centers are co-located.

satellite's travel over the exposure time. If the exposure time is suitably short such that the satellite does not leave the detector's field of view (FOV), the streak will have two endpoints. The angle between the two endpoints can be estimated by determining the image's scaling factor (the number of image pixels per degree in the sky) and then estimating the x-y pixel location of the two endpoints. The satellite's apparent angular velocity can then be estimated by dividing the estimated streak angle by the image's exposure time.

When assuming a circular orbit, a LEO satellite's apparent angular velocity observed at local zenith can be used to estimate the orbit's radius, which is also known as the semi-major axis (SMA). Using this assumption, the argument of perigee is undefined and the true anomaly can be defined from any convenient point in the orbit (such as the ascending node). Kepler's Third Law of Orbit Motion can assist in determining the satellite's period of orbit (and therefore its mean motion[3]) from the estimated SMA. Estimates of the satellite's orbit inclination[4] and its right ascension of the ascending node (RAAN)[5] can be made using the streak's orientation, based on its apparent direction of travel in the image and the image's orientation with respect to the equatorial coordinate system.

This paper proposes a simple method of initial orbit determination (IOD) using images of LEO satellites observed near the local zenith. The suggested equipment and setup procedure is presented in Section II. The derivation of the IOD equations and their conditions of use are presented in Section III. In Section IV, a number of comparisons between estimated LEO orbit elements extracted from CCD images and their most likely orbit elements (from TLEs) are presented and discussed.

## II Equipment and Setup

### A. Equipment

To obtain images of LEO satellites near the local zenith, a detector with a FOV greater than 5° is recommended. The lens should have a focal length of between 50mm and 200mm. The exposure time should be short enough so that the background stars will appear as points (not streaks) and long enough to show the satellite motion as streaks (not dots).

The detector should have the capability of recording the image's date and time to the nearest second or better. If the exposure time is set manually (for example, at the "bulb" (B) setting) the detector should have the ability to record the exposure time. The most convenient setup would be capable of automatically storing all images, including headers, to a digital storage device.

To obtain images with a CCD camera, CCD controlling software is essential. This software is normally included with a new CCD camera. For convenience, this software should also be able to read the images and display the x and y pixel values of the mouse cursor location within the image. If using a DSLR[6] or other retail digital camera, some image processing software is required in order to read the x and y pixel values from the images.

### B. Suggested Setup Procedure

The detector can be pointed to the local zenith by attaching it to a small and sturdy tripod and then placing a small bubble level on the camera body such that the apparatus can be leveled with the camera lens pointed towards the zenith. Although the detector's azimuthal (horizon) orientation is not particularly important, the orientation of the part of the lens corresponding to the top of an image can be roughly

[3] The mean motion is the reciprocal of the orbit period, typically stated in orbits·day$^{-1}$.
[4] Inclination refers to the orbit plane's angle with respect to the Earth's equatorial plane.
[5] RAAN is the right ascension (RA) coordinate of the intersection point of the orbit plane and the equatorial plane as the satellite crosses the equatorial plane from south to north.
[6] Digital Single Lens Reflex.

aligned with the true north (roughly towards Polaris' azimuth). This allows for easier identification of the streaks' orientations during image analysis.

When imaging the satellites, the camera should be as stationary as possible. A computer-controlled device (such as a CCD) is the most convenient detector because it can be controlled remotely with a computer interface. Remote control is also possible with a DSLR camera. If the camera cannot be remotely controlled, the shutter timer can be used to obtain images without having to push any buttons on the camera during exposure times.

It will not be immediately clear which satellites will be detectable during imaging. However, several online resources can predict when naked eye satellites will be observable, including the predicted times of their maximum elevations (90° being the local zenith). When using a computer controlled detector, it may be possible to automatically obtain and store images over several hours, thus creating an optical fence that will detect all suitably bright satellites that pass within its FOV. This optical fence will also serve to remove all bias with respect to choosing the most accessible satellite targets.

An exposure time of 5s or less is recommended because the satellite angular velocity at the local zenith can be as high as $3°\cdot s^{-1}$. It is not necessary to obtain one image after another as quickly as possible (maximum cadence); however, if the maximum amount of satellites is desired or if the FOV is under 5°, then a high cadence is recommended.

## III Derivations

The derivations are not recommended for secondary school students; however, the final results and their conditions can be used by students to estimate an orbit's SMA, inclination and RAAN from images of LEO satellites obtained near the local zenith.

The derivations required several important assumptions; the first, being a circular orbit (zero eccentricity). For the closer LEO satellites orbiting at less than 1,000km in altitude, this is not an unreasonable assumption, since a high eccentricity LEO orbit would necessarily intersect the Earth's surface and therefore, could not exist. The second assumption is that a satellite's transverse angular velocity is constant throughout its travels through the CCD FOV (when pointed at local zenith). This assumption also applies to the angular velocity estimated from a streak's endpoints. The third assumption is that the satellite's instantaneous equatorial coordinates correspond to the midpoint between the streak endpoints. The fourth assumption is that the observed satellite's altitude is the difference between its circular orbit radius and the Earth's radius at the observer's latitude.

### A. Semi-Major Axis

The SMA (a) is defined as the average of a satellite's perigee (closest) distance and its apogee (furthest) distance. When assuming a circular orbit, the SMA becomes a constant orbit radius. When observed near the local zenith, the satellite's tangential orbit velocity (v) is related to the satellite's apparent angular velocity ($\omega$) and its altitude above the observer (h) according to Eq. 1.

The satellite's tangential orbit velocity is also related to the SMA by Kepler's Third Law, shown in Eq. 2, which equates the centripetal acceleration with the gravitational acceleration, where $\mu$ is the Earth's gravitational parameter ($398{,}600.4418\ km^3\cdot s^{-2}$). The fourth aforementioned assumption that relates the satellite's SMA with its altitude is shown in Eq. 3, where $R_E$ is the Earth's radius at the observer's latitude [1].

$$v = h\omega \tag{1}$$

$$v^2 = \frac{\mu}{a} \tag{2}$$

$$a = h + R_E \tag{3}$$

Squaring Eq. 1, equating it with Eq. 2, and substituting Eq. 3 for the SMA yields Eq. 4 [1]. The three roots of Eq. 4 will be comprised of one positive real number (physically possible) and two negative real numbers (not physically possible). The positive real root of Eq. 4 can be determined with the Cubic Formula and DeMoivre's Theorem. Equation 3 can determine the corresponding SMA from the estimated altitude. The full analytical solution that determines the orbit's SMA is shown in Eq. 5. The only parameters required to solve Eq. 5 are $R_E$ (constant for a specific observation latitude) and ω.

$$h^3 + R_E h^2 - \frac{\mu}{\omega^2} = 0 \tag{4}$$

$$a = \frac{2R_E}{3}\left\{1 + \cos\left[\frac{1}{3}\cos^{-1}\left(\frac{27\mu}{2R_E^3\omega^2} - 1\right)\right]\right\} \tag{5}$$

In order to use Eq. 5, the satellite's angular velocity should satisfy the condition shown in Eq. 6. The minimum value is approximately 11.1'·s$^{-1}$, depending on the observer's latitude. The minimum angular velocity corresponds to a maximum SMA of approximately 8,500 km (2,120 km altitude), which can easily serve as an upper boundary for the majority of LEO satellites. If the angular velocity is less than 11.1'·s$^{-1}$, the solution of Eq. 5's arc-cosine term becomes imaginary and the hyperbolic cosine (cosh) is required. Since secondary school students will likely not be familiar with the concept of hyperbolic cosines, the limit shown in Eq. 6 should be recommended.

$$\omega \geq \sqrt{\frac{27\mu}{4R_E^3}} \tag{6}$$

A plot of the determined SMA versus the angular velocity according to Eq. 5 is shown in Fig. 1. The black dotted vertical line indicates the minimum angular velocity according to Eq. 6. The maximum angular velocity (3.0°·s$^{-1}$) roughly corresponds to the minimum possible LEO SMA. When the angular velocity is between 0.6°·s$^{-1}$ and 3.0°·s$^{-1}$, the slope is low and the SMA's uncertainty is also low (relative to the angular velocity uncertainty). For an angular velocity between 0.6°·s$^{-1}$ and 0.185°·s$^{-1}$, the slope greatly increases, thereby increasing the SMA's uncertainty.

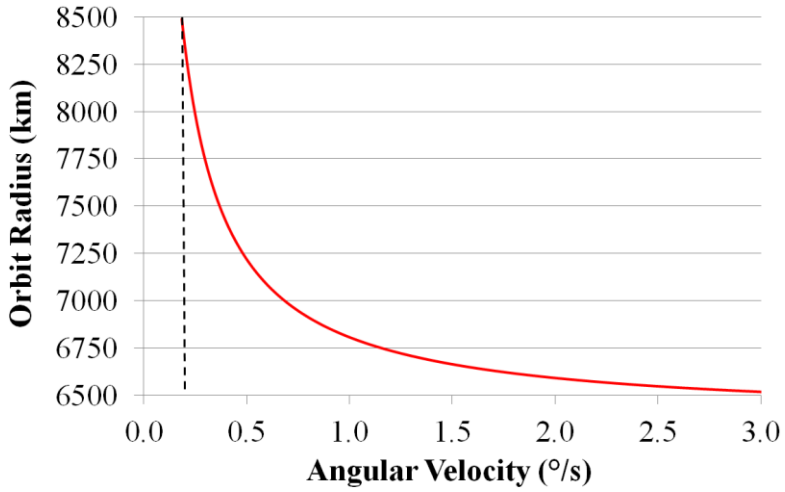


***Fig. 1.*** *SMA versus angular velocity.*

## B. Inclination

Inclination (i) is the angle between the orbit plane and the Earth's equatorial plane, as illustrated in Fig. 2(a). The inclination can have a value between 0° and 180°, where a value between 0° and 90° indicates a "prograde" orbit and a value between 90° and 180° indicates a "retrograde" orbit.

When it is observed at the local zenith, as illustrated in Fig. 2(b), a satellite will have some geocentric RA and declination (dec.) equatorial coordinates ($\alpha_{GC}$ and $\delta_{GC}$, respectively). A coordinate translation is typically required when converting from geocentric to topocentric equatorial coordinates or vice-versa. However, when the satellite is observed near the local zenith, the Earth's center (point C of Fig. 2(b)), the observer's location (point P of Fig. 2(b)), and the satellite's position are nearly in a straight line. In that case, the topocentric equatorial coordinates are approximately equal to the geocentric equatorial coordinates, as shown in Fig. 2(b). The satellite's RA coordinate will be at the angle $\gamma$ from the RAAN, as shown in Fig. 2(b) and Eq. 7.

The satellite's dec. coordinate can be expressed in terms of the inclination (i) and the $\gamma$ angle, as shown in Eq. 8. The reciprocal of Eq. 8 results in Eq. 9. Using trigonometric identities and rearranging terms, Eq. 9 can be simplified to yield Eq. 10.

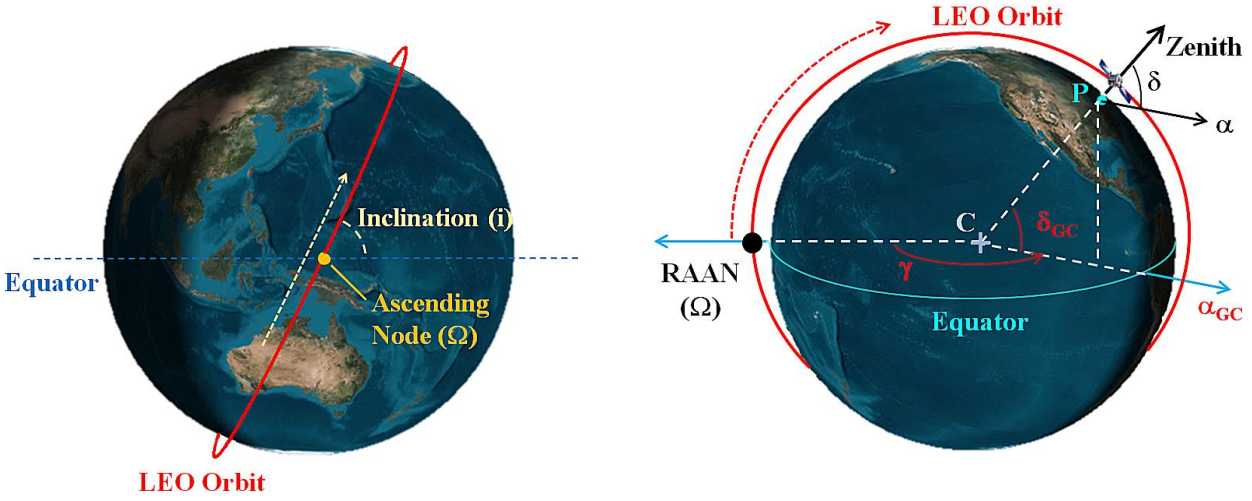


*a) Inclination and ascending node.* *b) Geocentric and topocentric RA and dec.*

***Fig. 2.*** *Inclination, ascending node, and equatorial coordinates.*

$$\gamma = \alpha - \Omega \tag{7}$$

$$\cos^2\delta = \frac{\cos^2 i}{1-\cos^2\gamma\sin^2 i} \tag{8}$$

$$\sec^2\delta = \sec^2 i - \cos^2\gamma\tan^2 i \tag{9}$$

$$\tan^2 i = \frac{\tan^2\delta}{\sin^2\gamma} \tag{10}$$

Equation 10 conveys information about a satellite's instantaneous position, but not its motion. The inclination can only be determined from a streak's orientation, which requires the rates of both the RA and dec. coordinates (or the "x" and "y" pixel rates) over the exposure time. Knowing the instantaneous rates of change of both RA and dec. would be ideal; however, this is not possible when an image with a

non-zero exposure time is provided. The "streak slope" can be substituted for these rates of change, as shown in Eq. 11. The streak slope is defined as the ratio of the difference of the streak's "y" coordinates to the difference of the streak's "x" coordinates. Both pixel differences are defined as the first coordinate in time subtracted from the second coordinate, as shown in Eq. 11.

The cosδ term in the streak slope of Eq. 11 is required because of the "x" coordinate. Since the celestial sphere is not a plane, the range of RA coordinates in an image's FOV will increase as the absolute declination increases by a factor of the reciprocal of cosδ. Therefore, the range of RA coordinates in a FOV will be the minimum at the celestial equator and the maximum (actually all possible RA coordinates) at either of the celestial poles.

$$\frac{\frac{d\delta}{dt}}{\frac{d\alpha}{dt}} = \frac{d\delta}{d\alpha} \approx \frac{\Delta\delta\cos\delta}{\Delta\alpha} \approx \frac{\Delta y\cos\delta}{\Delta x} = \frac{(y_2 - y_1)\cos\delta}{x_2 - x_1} \tag{11}$$

After taking the derivative of Eq. 10 (orbit inclination is constant in the short term), then substituting the streak slope for the rates of change, and rearranging terms, Eq. 12 results. Equations 10 and 12 can then be equated and rearranged to yield Eq. 13.

$$\tan^2 i = \frac{\tan\delta\sec\delta}{\sin\gamma\cos\gamma}\left[\frac{\Delta y}{\Delta x}\right] \tag{12}$$

$$\tan\gamma = \frac{\sin\delta}{\left[\frac{\Delta y}{\Delta x}\right]} \tag{13}$$

Equation 13 relates the satellite's RA angle from the RAAN (γ) to the dec. and the streak slope. Equation 13 can be expressed as a function of sinγ, as shown in Eq. 14. Equation 14 can then be substituted for $\sin^2\gamma$ in Eq. 10, yielding Eq. 15. When the satellite is observed near the local zenith, Eq. 15 relates the orbit inclination to the satellite's dec. coordinate and its streak slope.

$$\sin^2\gamma = \frac{\sin^2\delta}{\sin^2\delta + \left[\frac{\Delta y}{\Delta x}\right]^2} \tag{14}$$

$$\tan^2 i = \frac{\sin^2\delta + \left[\frac{\Delta y}{\Delta x}\right]^2}{\cos^2\delta} \tag{15}$$

Equation 15 will give a solution between the observer's latitude and 90°; however, the orbit could be retrograde (an inclination greater than 90°). Equation 16 states the condition required to determine the orbit inclination when the streak's Δx value is negative. When using radians, replace the 180° in Eq. 16 with π radians.

Figure 3 plots the inclination for streak slopes between -50 and 50 at an observer's latitude of 45°. The green lines indicate ascending (north to south) motion. The red lines indicate descending (north to south) motion. The arrows denote the apparent direction of travel in the image, assuming the detector is aligned with the equatorial coordinate system. For streak slopes greater than 5 and less than -5, the inclination

uncertainty will be small, relative to the slope uncertainty. For streak slopes between -5 and 5, the inclination uncertainty will be more sensitive to the slope uncertainty.

$$i(\Delta x < 0) = 180^{o} - \tan^{-1}\left\{\frac{\sqrt{\sin^2\delta + \left[\frac{\Delta y}{\Delta x}\right]^2}}{\cos\delta}\right\} \tag{16}$$

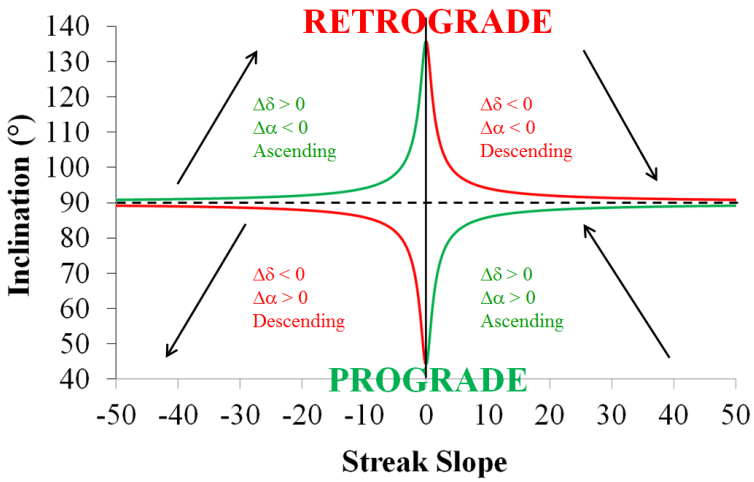


***Fig. 3.*** *Inclination versus streak slope.*

## C. Right ascension of the ascending node

Equation 13 determines the RA angle from the ascending node to the satellite's RA in the direction of ascending RA, as illustrated in Fig. 4. Substituting Eq. 7 into Eq. 13 and rearranging the result determines the RAAN, as shown in Eq. 17.

Equation 13 will give a solution for γ that is between -90° and 90°; however, γ can range from -180° to 180°. When the satellite is ascending (increasing dec.), then Eq. 17 can be used as-is. When the satellite is descending, then the condition shown in Eq. 18 is required. The "±" in Eq. 18 refers to a streak with an increasing (+) x pixel value or a decreasing (-) x pixel value, corresponding to a -180° or a +180° correction, respectively (∓ 180°). When using radians, replace the 180° in Eq. 18 by π radians.

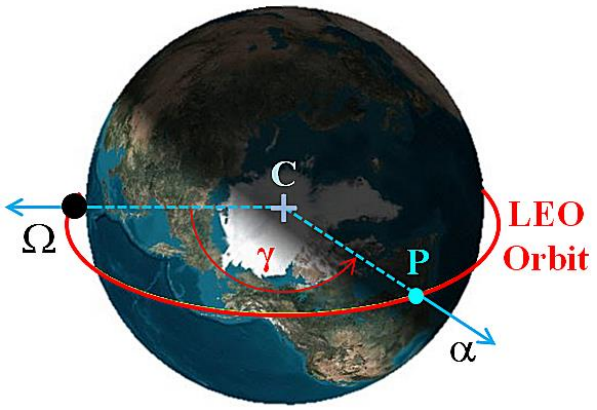


***Fig. 4.*** *The γ angle from ascending node to the satellite at zenith.*

$$\Omega = \alpha - tan^{-1}\left\{\frac{sin\,\delta}{\left[\frac{\Delta y}{\Delta x}\right]}\right\} \tag{17}$$

$$\Omega(\Delta y < 0, \pm\Delta x) = \mp 180^{o} + \alpha - \tan^{-1}\left[\frac{\sin\delta}{\left(\frac{\Delta y}{\Delta x}\right)}\right] \tag{18}$$

Figure 5 shows the γ angle for streak slopes between -50 and 50 at an observer latitude of 45°. The green lines indicate ascending (north to south) motion. The red lines indicate descending (north to south) motion. The arrows denote the apparent direction of travel in the image when the detector is aligned with the topocentric equatorial coordinate system. For streak slopes greater than 3 and less than -3, the γ angle uncertainty will be small, relative to the slope uncertainty. For streak slopes between -3 and 3, the γ angle uncertainty will be more sensitive to the slope's uncertainty.

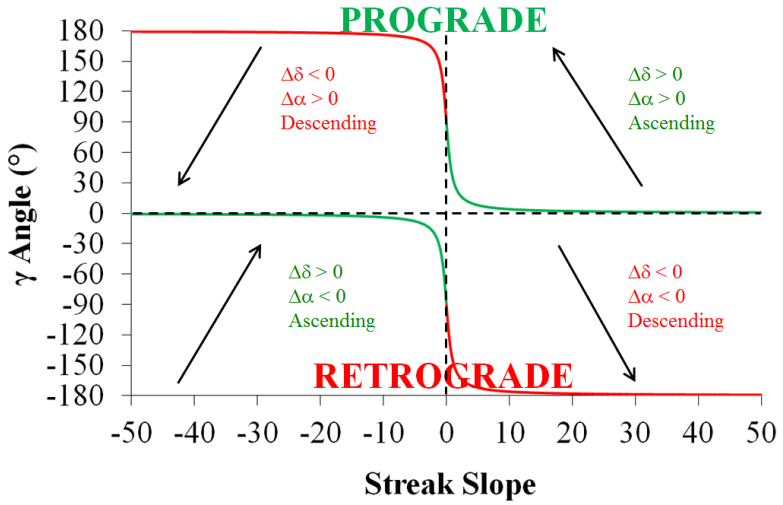


***Fig. 5.*** *γ angle versus streak slope.*

## IV Results

From 00:18 to 03:34 UTC April 6, 2016, a single SBIG[7] model ST-9XE CCD camera fitted with a 50mm focal length Rikenon lens set at f/2 was pointed at the local zenith from a location of longitude -76° 34' 08"[8] and geodetic latitude 44° 12' 49" to conduct a survey of all detectable LEO satellites that passed within 5° of the local zenith. A total of 51 satellites were positively detected and correlated, 27 of which were selected for IOD with the Zenith Method. For each orbit element, the TLE values ($a_{TLE}$, $n_{TLE}$, $i_{TLE}$, and $\Omega_{TLE}$) were extracted from TLEs with epochs that were the closest to the observation epoch. The $\Omega_{TLE}$ values were extracted from TLEs propagated to the imaging time in order to minimize the secular precession effects.

Table 1 compares the orbit element estimation results and their corresponding TLE values, in order of

[7] Santa Barbara Instrument Group
[8] A negative longitude indicates a meridian west of Greenwich.

ascending TLE SMA. The final satellite listed in the table had an orbit radius of over 8,500km and therefore had an angular velocity less than $11' \cdot s^{-1}$. Its SMA was therefore estimated with the hyperbolic cosine version of Eq. 5.

***Table 1.*** *Estimated versus TLE LEO orbit elements.*

| #[9] | Common Name | a (km) | $a_{TLE}$ (km) | n ($d^{-1}$) | $n_{TLE}$ ($d^{-1}$) | i (°) | $i_{TLE}$ (°) | Ω (°) | $\Omega_{TLE}$ (°) |
|---|---|---|---|---|---|---|---|---|---|
| 29508 | CZ-4 Debris | 6797.5 | 6809.6 | 15.491 | 15.450 | 97.3 | 97.7 | 136.5 | 133.2 |
| 39195 | SL-27 R/B | 6845.7 | 6854.7 | 15.328 | 15.298 | 79.0 | 74.7 | 314.8 | 322.9 |
| 19046 | SL-3 R/B | 6900.4 | 6939.4 | 15.146 | 15.018 | 97.4 | 97.6 | 153.0 | 148.8 |
| 36088 | SJ-11-01 | 7053.0 | 7071.9 | 14.657 | 14.598 | 97.9 | 98.2 | 143.5 | 145.2 |
| 24792 | Iridium-8 | 7158.2 | 7155.8 | 14.335 | 14.342 | 86.0 | 86.4 | 138.4 | 141.2 |
| 09443 | Cosmos-858 | 7121.5 | 7156.5 | 14.303 | 14.340 | 74.6 | 74.0 | 132.3 | 130.5 |
| 08027 | SL-3 R/B | 7197.4 | 7229.7 | 14.218 | 14.073 | 80.8 | 81.2 | 117.1 | 116.5 |
| 39228 | SL-24 R/B | 7444.7 | 7251.0 | 13.515 | 14.061 | 97.7 | 97.5 | 139.3 | 141.0 |
| 02828 | GGSE-4 | 7221.0 | 7281.2 | 14.148 | 13.973 | 69.4 | 70.0 | 137.0 | 136.0 |
| 10702 | Landsat-3 | 7269.9 | 7283.6 | 14.006 | 13.966 | 99.1 | 98.9 | 141.4 | 137.6 |
| 24773 | SL-8 R/B | 7373.0 | 7364.9 | 13.713 | 13.736 | 87.4 | 82.9 | 330.5 | 337.4 |
| 07008 | Cosmos-627 | 7413.8 | 7367.6 | 13.600 | 13.728 | 87.3 | 83.0 | 344.5 | 346.2 |
| 05050 | Cosmos-400 | 7537.9 | 7370.1 | 13.266 | 13.721 | 70.4 | 65.8 | 351.9 | 351.4 |
| 40341 | CZ-4C R/B | 7166.3 | 7381.4 | 14.311 | 13.690 | 62.7 | 63.5 | 111.5 | 112.9 |
| 00447 | Thor Ablestar R/B | 7305.2 | 7491.1 | 13.904 | 13.390 | 50.5 | 50.1 | 21.6 | 32.1 |
| 40878 | Yaogan-27 | 7555.0 | 7578.4 | 13.221 | 13.160 | 101.1 | 100.5 | 163.2 | 158.0 |
| 39410 | Yaogan-19 | 7524.3 | 7582.2 | 13.133 | 13.150 | 100.0 | 100.4 | 167.4 | 170.3 |
| 06320 | SL-8 R/B | 7726.2 | 7732.0 | 12.784 | 12.769 | 78.8 | 74.0 | 347.0 | 354.7 |
| 31571 | Globalstar-M065 | 7543.1 | 7791.8 | 13.252 | 12.623 | 54.9 | 52.0 | 9.8 | 13.6 |
| 04320 | ITOS-1 (Tiros-M) | 7788.8 | 7834.1 | 12.630 | 12.520 | 101.0 | 101.9 | 158.2 | 159.2 |
| 08184 | Thorad Delta 1 Debris | 7785.3 | 7842.8 | 12.638 | 12.475 | 102.0 | 101.7 | 170.1 | 166.2 |
| 39484 | Cosmos-2489 | 7925.5 | 7872.6 | 12.305 | 12.429 | 86.9 | 82.5 | 321.0 | 329.6 |
| 10288 | Cosmos-942 | 7890.9 | 7875.4 | 12.385 | 12.422 | 74.0 | 74.0 | 139.6 | 141.8 |
| 16910 | H-1 R/B (Mabes) | 7593.7 | 7916.4 | 13.120 | 12.326 | 47.0 | 50.0 | 100.3 | 96.3 |
| 13168 | SL-8 R/B | 7933.2 | 7958.2 | 12.287 | 12.229 | 78.8 | 74.1 | 351.6 | 359.4 |
| 25962 | Globalstar-M034 | 7883.9 | 8152.7 | 12.402 | 11.794 | 53.1 | 52.0 | 103.9 | 102.2 |
| 41108 | Fregat Debris (Tank) | 8806.2 | 8612.1 | 10.506 | 10.863 | 50.5 | 50.4 | 3.7 | 9.3 |

The satellite's altitude does appear to have some effect on the estimated SMA. Generally, the higher altitude satellites will have smaller streaks (for a specific CCD FOV and exposure time) and they would be more susceptible to the streak length uncertainty. The two highest altitude satellites listed in Table 1 have estimated SMAs that differ from their respective TLE values by several hundred kilometers. Globalstar-M034's estimate was approximately 300km less than the TLE value, while the Fregat Debris' estimate was approximately 200km greater than the TLE value. The SMA versus angular velocity plot shown in Fig. 1 does not include a SMA greater than 8,500km; however, it does suggest that the SMA uncertainty becomes more sensitive to the angular velocity uncertainty for SMAs that are greater than 7,000km. Table 1 seems to confirm this hypothesis. For example, all satellites with SMAs less than 7,200km appear to have estimates within 50km of their TLE values. Satellites with SMAs greater than 7,200km can have differences as large as several hundred kilometers from their corresponding TLE values.

[9] The NORAD catalog number

For the most part, the estimated inclinations in Table 1 are all within a degree of their corresponding TLE values. This was unexpected, especially when considering the higher slopes between inclinations of 45° and 85° in Fig. 3. The five satellites with inclinations between 50° and 53° had estimations within 3° of their TLE values. However, several satellites with inclinations between 65° and 80° had estimations within 6°. There does not seem to be any correlation between the estimated inclination difference from the TLE value and the satellite's altitude.

The majority of the estimated RAANs appear to be within 3° of their corresponding TLE values. This might be due to the choice of the satellite's RA (midpoint of the streak). This was also unexpected, since Fig. 5 indicated that the RAAN estimate uncertainty would become more sensitive to the slope uncertainty at $\gamma$ angles between 15° and 165° and between -15° and -165°, which are the majority of the $\gamma$ angles. As seen with the inclination estimates, there does not seem to be any correlation between the estimated RAAN difference from the TLE value and the satellite's altitude.

## V Conclusions

The Zenith Method can estimate a LEO satellite's SMA, inclination and RAAN when it is observed at the local zenith. The method appears to be more reliable for those LEOs orbiting at less than 850km in altitude. The estimates of inclination and RAAN at any LEO altitude do appear to be more accurate than predictions might suggest.

From a secondary school student's perspective, the Zenith Method of IOD would appear to be a powerful, yet relatively simple, orbit determination tool. At face value, a LEO satellite's SMA, inclination, and RAAN can be determined very quickly and somewhat accurately by simply estimating its streak endpoints, determining its angular velocity and its streak slope, and then ''plugging'' these values into the equations shown in this paper. The real test of this method is not how well the orbit elements compare with the TLE values but if the satellite can be relocated at some future time when propagating the estimated elements.

The most important objective of the Zenith Method is to provide secondary school students with the tools required to understand the basics of satellite orbital mechanics; including, orbit determination and orbit propagation. When using this method, students should quickly realize that several important orbit elements are missing; namely the eccentricity, argument of perigee and the mean (or true) anomaly. They should also quickly find that being contained to the local zenith is very confining and the inevitable question should be asked: "Can orbit determination be performed when not observing satellites at the local zenith?'' Gauss' method and more accurate statistical methods (including the concept of residuals) may then be introduced. Students should be made aware that although the Zenith Method is not a perfectly accurate orbit determination tool; all orbit determination methods are based on measurements containing uncertainties.

The Zenith Method is a bridge between basic science and algebra and the space surveillance infrastructure that monitors the satellite population and protects it from harm. By observing real orbiting satellites and estimating their orbit elements using the Zenith Method, students are introduced to orbit determination in a user-friendly and practical manner. The Zenith Method can motivate students to learn more about the exciting adventures of orbit propagation and orbit determination and to eventually pursue a career in the space sciences.

## References

[1] Earl, M.A., "Determining the orbital height of a low-earth-orbiting artificial satellite observed near the local zenith," *Journal of the Royal Astronomical Society of Canada*, Vol. 100, No. 5, October 2006, pp. 199–203.